Mechanical Stabilization of Helical Chirality in a Macrocyclic Oligothiophene

SCHOLARONE™
Manuscripts

Mechanical Stabilization of Helical Chirality in a Macrocyclic Oligothiophene

Kevin J. Weiland[a], Thomas Brandl[a], Kenneth Atz[a], Alessandro Prescimone[a], Daniel Häussinger[a], Tomáš Šolomek[a] and Marcel Mayor*[a,b,c]

a) Department of Chemistry, University of Basel, St. Johanns-Ring 19, 4056 Basel (Switzerland)

b) Institute for Nanotechnology (INT), Karlsruhe Institute of Technology (KIT), P. O. Box 3640, 76021 Karlsruhe (Germany)

c) Lehn Institute of Functional Materials, School of Chemistry, Sun Yat-Sen University, Guangzhou 510274 (China)

ABSTRACT: We introduce a design principle to stabilize helically chiral structures from an achiral tetrasubstituted [2.2]paracyclophane by integrating it into a macrocycle. The [2.2]paracyclophane introduces a three-dimensional perturbation into a nearly planar macrocyclic oligothiophene. The resulting helical structure is stabilized by two bulky substituents installed on the [2.2]paracyclophane unit. The increased enantiomerization barrier enabled the separation of both enantiomers. The synthesis of the target helical macrocycle **1** involves a sequence of halogenation and cross-coupling steps and a high-dilution strategy to close the macrocycle. Substituents tuning the energy of the enantiomerization process can be introduced in the last steps of the synthesis. The chiral target compound **1** was fully characterized by NMR spectroscopy and mass spectrometry. The absolute configurations of the isolated enantiomers were assigned by comparing the data of circular dichroism spectroscopy with TD-DFT calculations. The enantiomerization dynamics was studied by dynamic HPLC, variable temperature 2D exchange spectroscopy and supported by quantum-chemical calculations.

INTRODUCTION

Helically chiral aromatic molecules,[1-3] besides their esthetic beauty, often possess interesting chiroptical properties such as intense circular dichroism or spin-selective electron transport.[4-6] Apart from ubiquitous helicenes, [2.2]paracyclophane (PC)[7,8] represents an interesting building block to form helical structures because tetrasubstituted PCs, prepared initially by *Hopf* and co-workers, are chiral. For instance, *Chujo* and coworkers demonstrated the synthesis of enantiopure doubly-helical macrocycles and discovered their intense chiroptical effects,[9,10] which were concluded to arise from the rigid geometry of the propeller-shaped molecules.

Our interest in "loop-shaped" helically chiral model compounds arises from their potential physical properties in single-molecule junctions. To investigate the suitability of the PC synthon, an achiral PC derivative was recently analyzed in a single-molecule junction displaying mechanically triggered conductance variations.[11] As the next step, we decided to investigate the PC building block as a helicity-inducing subunit in macrocycle **2b** (figure 1). We found the helically chiral molecule to enantiomerize rapidly in solution and therefore decided to stabilize the helical chirality by mechanically hindering the racemization through strategic installation of bulky substituents.[12]

Disconnection of a C–C bond between two thiophenes in a planar oligothiophene macrocycle (figure 1b) and attaching each of the termini to the pseudo-*para*-position of the top and the bottom benzene ring in PC, respectively, introduces a step in the macrocyclic ring, from which the helicity of the resulting PC macrocycle emanates (figure 1c,d). The oligothiophene macrocycle **2b** (figure 1d) com-
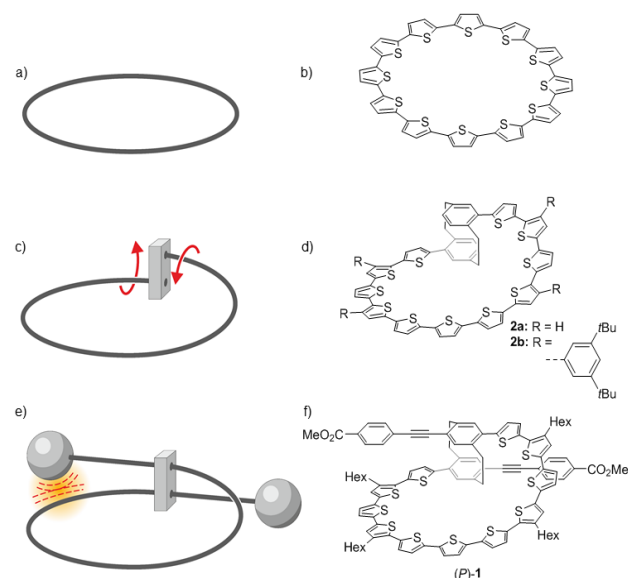
Figure 1. Development of the design of the mechanically stabilized helical chiral PC-macrocycle **1**. Starting from the planar ring (a) represented by cyclo[12]thiophene (b), the introduction of a step results in a helical chiral object (c) as in the oligothiophene macrocycle **2** comprising a PC subunit (d). Additional decoration of the PC subunit with bulky substituents hinders its enantiomerization by rotation of the PC subunit as sketched in (e). The concept is realized with the macrocyclic model compound **1** reported here.

prising a pseudo-*para* PC step was first assembled sequentially to determine the number of thiophene subunits required to close the macrocycle.[12] Such chiral macrocycles follow an enantiomerization

process described first by *Kurt Mislow* as "Euclidean rubber glove".[13–15] This means that during the entire enantiomerization process the object remains chiral and achiral arrangements can't be adopted without breaking a bond. The process resembles the transformation of a right-handed rubber glove into a left-handed one by turning it inside out. In the case of **2**, spontaneous enantiomerization was observed at room temperature due to rotation of the PC subunit around the single bonds integrating it into the oligothiophene macrocycle.[12]

Introduction of bulky rod-like arms with a bis-(*para*)-pseudo-*para* orientation[16] to the PC (figure 1e,f) should gear its free rotation, and thereby allow the separation of the enantiomers. To estimate the dimensions of the target structure **1**, the geometry of one enantiomer, based on the smallest unstrained cyclo[12]thiophene with one thiophene unit replaced by the substituted PC, was optimized by DFT and is depicted as Fig. S1.[17,18] The calculated distance between the carboxylic oxygen atoms is ~21 Å, while the largest distance between two sulfur atoms in the macrocycle is ~13.5 Å (figure S1). For the enantiomerization to occur, one of the *para*-ethynyl methylbenzoates must pass through the ring of the macrocycle, like a thread through the eye of a needle. We employed a similar strategy in the synthesis of a molecular turnstile, where a size mismatch of a push-pull rod and a conjugated macrocyclic ring was used to stabilize atropisomers through hindered rotation.[19]

DISCUSSION

The synthesis (scheme 1) of target macrocycle **1** started from the literature-known dimethyl 7,13-dibromo[2.2] paracyclophane-4,16-dicarboxylate and trimethyl(5-(4,4,5,5-tetramethyl-1,3,2-dioxaborolan-2-yl)thiophen-2-yl)silane (**3**) which were coupled under *Suzuki-Miyaura* conditions.[16,20] Conversion of the trimethylsilyl-group of **4** to bromine proceeded in high yield but had to be performed in dimethylformamide at 70 °C since the obtained building block **5** was poorly soluble in other common solvents. Subsequently, **5** was reacted under Pd-PEPPSI™-IPr catalysis with 3-hexylthiophene-2-boronic acid pinacol ester yielding tetrathiophene **6**. Suitable crystals for single-crystal X-ray analysis of **6** (Fig. S18) were obtained from a dichloromethane (DCM) ethanol mixture. The methyl esters of **6** were then reduced with diisobutylaluminiumhydride (DIBAL-H) and subsequently oxidized with *Bobitt's* salt to give dialdehyde **7**. It was necessary to control the amount of DIBAL-H precisely, because more than four equivalents of the reagent led to complex product mixtures. Halogenation of **7** leads to a poorly soluble intermediate, which was directly reacted with **3** under Pd-PEPPSI™-IPr catalysis to give hexathiophene **8**. Conversion of the TMS groups of **8** to the corresponding dibromide yielded **9** in excellent yield. Next, building block **12** was assembled from triisopropyl(thiophene-2-ylethynyl)silane, which was converted to pinacol-boronic ester **10**. *Suzuki-Miyaura* coupling afforded intermediate
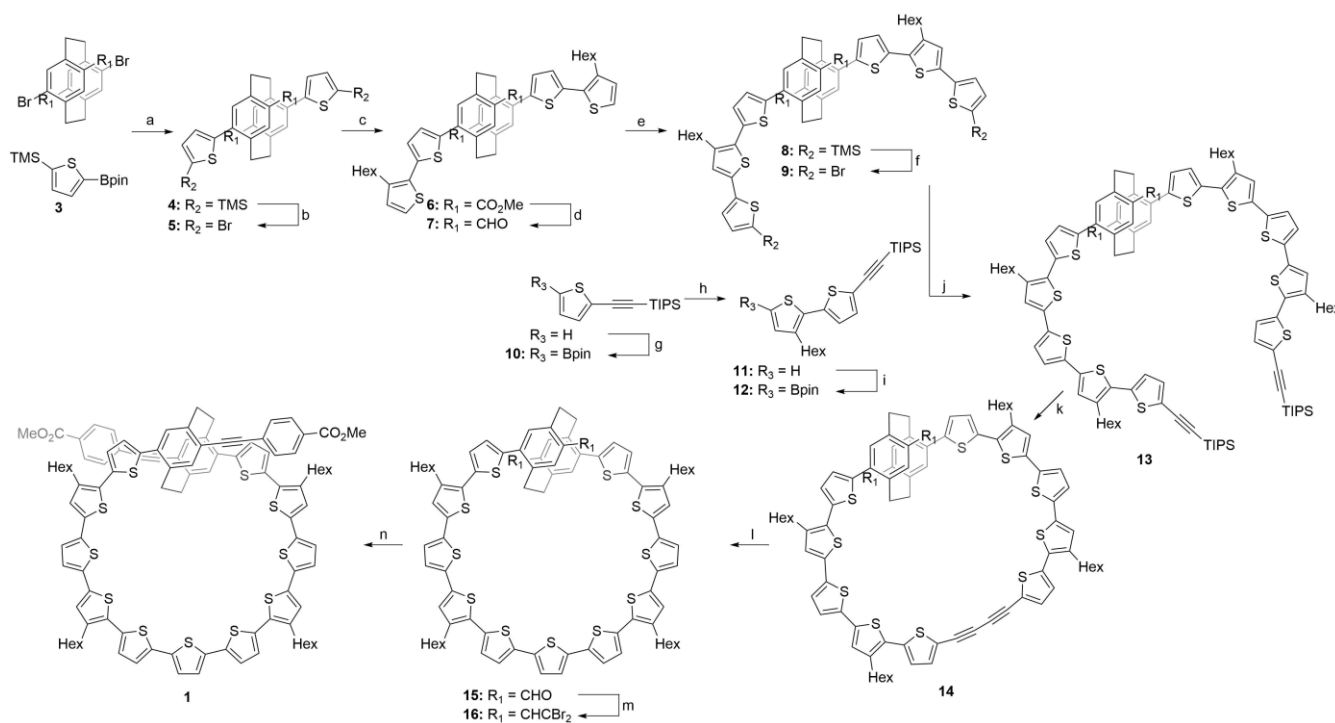

Scheme 1. Synthesis of target compound **1**. Reaction conditions: a) **3**, Pd(dppf)Cl₂, K₃PO₄, toluene/H₂O 10:1, 2 h, 110 °C, 83%; b) NBS, DMF, 70 °C, 18 h, 93%; c) 3-hexylthiophene-2-boronic acid pinacol ester, Pd-PEPPSI™-IPr, K₂CO₃, toluene/MeOH 1:1, 70 °C, 20 min, 81%; d) 1. DIBAL-H, THF, 0 °C, 3 h; 2. *Bobitt's* salt, silica gel, CH₂Cl₂, rt, 18 h, 79%; e) 1. NBS, CHCl₃, rt, 18 h; 2. **3**, Pd-PEPPSI™-IPr, K₂CO₃, toluene/MeOH 1:1, 70 °C, 30 min, 89%; f) NBS, AcOH/CHCl₃ 1:1, rt, 16 h, 99%; g) *n*-BuLi, 2-isopropoxy-4,4,5,5-tetramethyl-1,3,2-dioxaborolane, THF, -78 °C to rt, 18 h, 99%; h) 2-bromo-3-hexylthiophene, Pd-PEPPSI™-IPr, K₂CO₃, toluene/MeOH 1:1, 70 °C, 20 min, 51%; i) *n*-BuLi, THF, 2-isopropoxy-4,4,5,5-tetramethyl-1,3,2-dioxaborolane, -78 °C to rt, 18 h, 97%; j) Pd-PEPPSI™-IPr, K₂CO₃, toluene/MeOH 1:1, 70 °C, 30 min, 72%; k) 1. TBAF, THF_aq, 16 h; 2. CuCl, Cu(OAc)₂, pyridine, 80 °C, 40 h (syringe pump), 85%; l) Na₂S · 9 H₂O, DMF/2-methoxyethanol 1:1, 122 °C, 2h, 94%; m) CBr₄, PPh₃, CH₂Cl₂, 0 °C, 1 h, 80%; n) 1. LDA, THF, 0 °C to rt; 2. methyl-4-iodobenzoate, Pd(PPh₃)₄, CuI, THF, diisopropylamine, 55 °C, 2 h, 18%.

11, which was converted to pinacolboronic ester **12**. Another *Suzuki-Miyaura* reaction of **12** and **9** afforded decathiophene **13**, which was first deprotected with tetrabutylammonium fluoride and subjected directly to modified *Eglinton* coupling conditions. Macrocycle **14** was obtained in excellent yield of 85% and was reacted with Na$_2$S to give undecathiophene macrocycle **15** that contains all eleven thiophene units of the target compound **1**. The rod-like arms were installed by treating **15** with the *Corey-Fuchs* reaction sequence,[21] converting the dialdehyde into the diacetylene, which was directly subjected to *Sonogashira-Hagihara* coupling conditions with 4-iodomethylbenzoate to yield the target molecule **1** that was purified by recycling gel permeation chromatography in chloroform after aqueous work-up. Compound **1** showed prolonged stability to air and light as a solid. It was characterized by ^{1}H, as well as 2D NMR and UV/Vis spectroscopy, and high-resolution MALDI-TOF spectrometry (see the supporting information). Notably, the ^{1}H NMR spectrum showed two separate resonances of the two methyl esters, indicating that the enantiomerization is slow on the timescale of the NMR experiment. The isotopic pattern recorded in the MALDI-TOF mass spectrometry experiment matched the elemental composition of **1** ([M]$^+$ C$_{104}$H$_{98}$O$_4$S$_{11}$).

The enantiomers of **1** were separated by HPLC on a chiral stationary phase (Chiralpak IG, eluent ethylacetate/*n*-hexane 1:4, 1.0 mL min^{-1}, column oven: T = 18 °C). The isolated fractions of enantiomers displayed identical MALDI-TOF mass spectra and mirror images of their electronic circular dichroism (ECD) spectra with a set of *Cotton* effects at 265, 283, 298, 333, 364, 408, 457, and 536 nm (figure 2a). The *Cotton* effects are of low intensity compared with e.g. those observed for doubly-helical PC macrocycles of Chujo and coworkers,[22,23] which probably reflects the high flexibility of the PC unit in the oligothiophene macrocycle. It should be noted that despite all precautions (see experimental section) a partial racemization of the samples could occur during the course of the ECD measurements. The absolute configuration of the enantiomers was revealed by simulation of the ECD spectra with TD-DFT calculations

(see supporting information (SI)) that allowed to assign the (*M*)- and the (*P*)-configuration to the first and the second eluted fraction, respectively, in the chiral HPLC separation (figure 2b).[24,25]

Reinjection of an initially pure enantiomer of **1** stored at room temperature (rt) for several minutes already displayed the appearance of the other enantiomer, pointing at racemization at rt in spite of the length of the rod-like arms which were mounted to hinder the PC rotation. Thus, the enantiomerization behavior of **1** was investigated by means of dynamic variable temperature (VT) HPLC on a chiral stationary phase. The elution profiles of **1** in the temperature range from 293 to 328 K in steps of 5 K (eluent ethylacetate/*n*-hexane 2:3) was recorded and analyzed (see SI) with the DCXplorer[26] and the dHPLC Y2K[27,28] software packages. We found the half-life of enantiomerization is only $t_{1/2}^{298K}$ = 15.9 ± 0.5 min at 298 K with the activation free energy calculated as $\Delta G^{\ddagger}_{298K} \approx 91$ kJ mol^{-1} by both programs. The VT HPLC experiments further allowed for constructing an *Eyring* plot to dissect the free energy barrier into the corresponding enthalpy ($\Delta H_e^{\ddagger} \approx 37$–42 kJ mol^{-1}), and entropy ($\Delta S_e^{\ddagger} < -160$ J mol^{-1}K^{-1}) contributions. The values determined for $\Delta H_e^{\ddagger}$ and $\Delta S_e^{\ddagger}$ are striking because they suggest that the PC rotation is to a large extent controlled by a vast entropic penalty. Considering the size of the macrocycle **1** and the length and the stiffness of the methyl 4-ethynylbenzoate arms, the $\Delta H_e^{\ddagger}$ values appear to be intriguingly
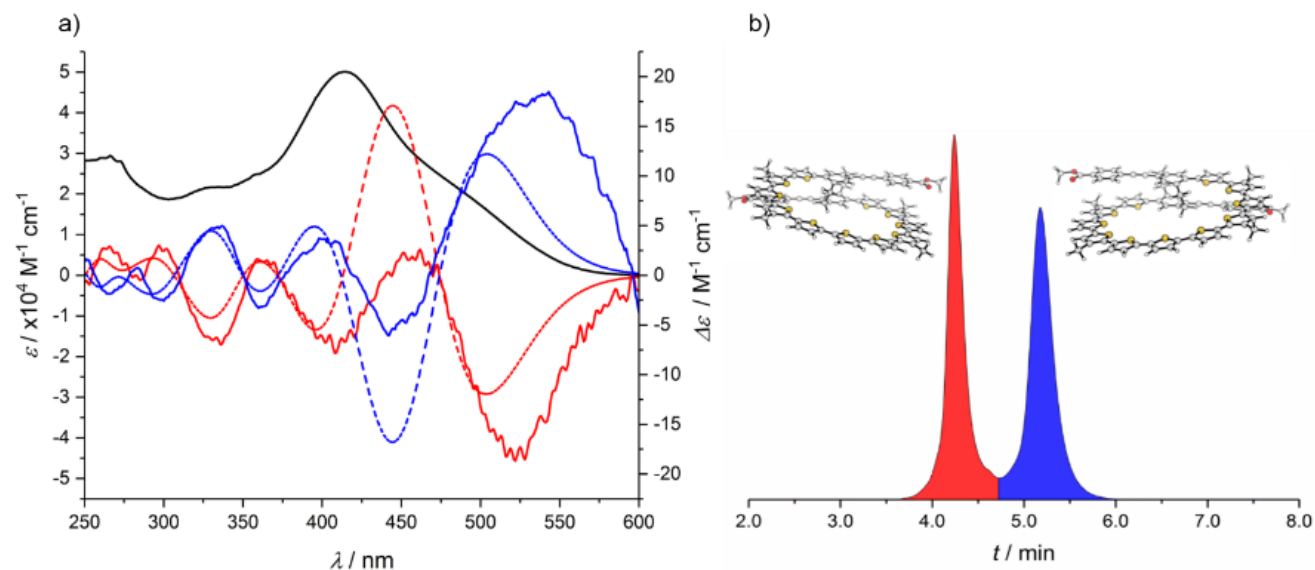
Figure 2. a) UV/Vis spectrum (black line) of a DCM solution of **1**, experimental (solid lines; recorded at 10 °C in *n*-hexane/EtOAc 4:1) and calculated (dashed lines) ECD spectra of (*M*)-**1** (red) and (*P*)-**1** (blue). b) Representative elution profile from the VT HPLC experiment (298 K column temperature, detected at 409 nm): (*M*)-**1** (red area) and (*P*)-**1** (blue area). The model shows the absolute configuration (the hexyl chains are replaced with methyl groups for clarity).
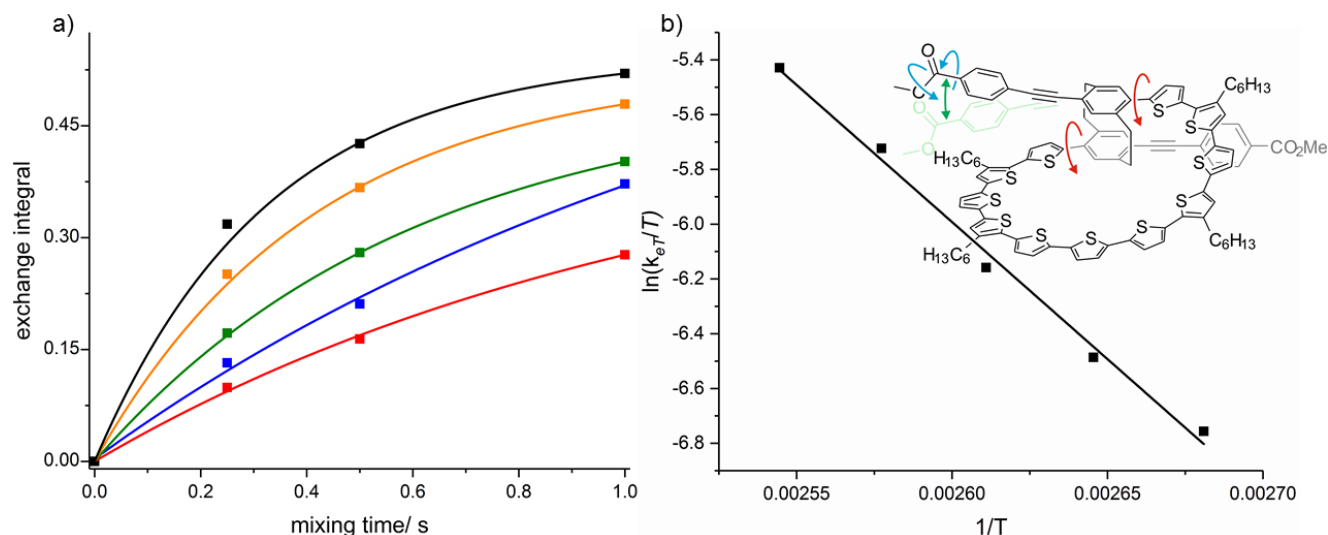
Figure 3. a) Exchange integral against mixing time in the VT EXSY experiment (red: 373 K, blue: 378 K, green: 383 K, orange: 388 K, black: 393 K). b) *Eyring* plot from data obtained from VT EXSY experiment. Linear fit to the data provides the enthalpy ($\Delta H_e^{\ddagger}$ = 83 kJ mol^{-1}) and the entropy ($\Delta S_e^{\ddagger}$ = −31 J mol^{-1} K^{-1}) for the racemization process. The arrows indicate specific geometric changes obtained from calculations (red: PC rotation, green: arm bending, blue: methoxy or carboxylate rotations).

low. The preexponential factor $\log(A) \approx 5$ ($E_a \approx 45$ kJ mol^{-1}) for enantiomerization of **1**, which is a unimolecular process, obtained from *Arrhenius* analysis suggests that the temperature dependence of the rate constant obtained from the elution profile analysis may be inaccurate. Indeed, it has been described previously that the elution profile analysis from dynamic VT HPLC experiments provides accurate values of activation free energy but tends to overestimate the entropy contribution when compared to alternative methods like dynamic ECD, VT NMR spectroscopies, or quantum-chemical calculations.[29] Possibly, the heterogenous nature of the HPLC experiment, where equilibria of the analyte with the chiral stationary phase are involved, results in enthalpy–entropy compensation affecting the individual activation parameters. As alternative access to these values, a 1,1,2,2-tetrachloroethane-d_2 solution of racemic **1** was studied by VT 2D exchange spectroscopy (EXSY) in a temperature range of 373–393 K in steps of 5 K (see figure 3a and SI) to determine the rate constants. Indeed, in agreement with our expectation, an enthalpy dominated racemization process was monitored with $\Delta H_e^{\ddagger}$ = 83 kJ mol^{-1} and $\Delta S_e^{\ddagger}$ = −31 J mol^{-1} K^{-1} obtained from the corresponding *Eyring* plot (figure 3b). The activation free energy at 298 K however, was with $\Delta G^{\ddagger}_{298K}$ = 92.4 kJ mol^{-1} comparable with the value obtained by the dynamic VT HPLC experiments.

We performed quantum-chemical calculations to get a deeper insight into the enantiomerization mechanism. The size and the flexible nature of macrocycle **1**[30] coerced us to use a combination of semiempirical and DFT calculations (see SI for detailed description) at the PM6 and B3LYP level of theory, respectively. First, we performed a PM6 relaxed potential energy surface scan (PES scan) for **1** along the dihedral angle α that is defined as the angle between the planes of the PC benzene rings and those of the two adjacent thiophene units to mimic the PC rotation.[31] Note that clockwise and anticlockwise PC rotations are not equivalent because **1** is chiral. In any case, we discovered few possible enantiomerization pathways that all require (i) a considerable turn of PC from its energy minimum geometry, (ii) bending of the *para*-ethynyl methylbenzoate arm, and,

unexpectedly, (iii) a rotation of either (a) the methyl carboxylate by ~180° or (b) the methoxy group from its more stable *s-cis* to *s-trans* conformation. The latter processes (iii-a,b) decrease the steric repulsion between the methyl carboxylate and the thiophene macrocycle and are inevitable to complete the full PC turn required for enantiomerization. All our attempts to find a transition state for the enantiomerization of (*M*)- or (*P*)-**1** failed. We found that the energy range of the region of the PM6 PES where we observed the arm to successfully thread through the macrocycle during the constrained optimization was ~94–103 kJ mol^{-1} (figures S16 and S17). This energy range represents, neglecting the heat capacities, the upper boundary of the activation enthalpy, and it is in far better agreement with the VT EXSY experimental data than with that obtained from the VT HPLC. Additional evidence can be obtained by considering the energy cost of each of the processes (i-iii) separately assuming their additivity. This allowed us to use the higher-level B3LYP calculations (see SI for details) to obtain the PC rotation profile (figure S12) for the parent PC macrocycle **2a** (figure 1d). Again, an identical dihedral angle α for the two thiophene units was assumed. The calculated activation energy of ~35 kJ mol^{-1} (at 0 K) for the PC rotation is in very good agreement with the VT NMR activation free energy determined for **2b** ($\Delta G^{\ddagger}_{298K}$ = 38 kJ mol^{-1}).[12]

Constraining the valence and dihedral angles of the bent acetylene unit in the *para*-ethynyl methylbenzoate arm from the PM6 PES scan while relaxing all other internal coordinates provided (figure S13b) a penalty of ~26 kJ mol^{-1} for process (ii). Finally, rotation (iii-a) and (iii-b) in *para*-ethynyl methylbenzoate was computed[32-34] to require an activation energy of ~21 and ~28 kJ mol^{-1}, respectively. Addition of the individual contributions (i-iii) provides a semiquantitative estimate for the enantiomerization enthalpy of ~82 – 89 kJ mol^{-1} in very good agreement with our VT EXSY experiments data, suggesting that the enantiomerization of **1** is predominantly controlled by enthalpy.

CONCLUSION

1
2
3
4
5
6
7
8
9
10
11
12
13
14
15
16
17
18
19
20
21
22
23
24
25
26
27
28
29
30
31
32
33
34
35
36
37
38
39
40
41
42
43
44
45
46
47
48
49
50
51
52
53
54
55
56
57
58
59
60

In summary, we designed and synthesized a helically chiral oligothiophene macrocycle, chirality of which emerges from the incorporated [2.2]paracyclophane. The fast enantiomerization is prevented by employing bulky rod-like arms on the central [2.2]paracyclophane unit that allowed to resolve and characterize the chiroptical properties of individual enantiomers by ECD spectroscopy and DFT calculations. The dynamic variable temperature HPLC and 2D exchange spectroscopy permitted to obtain the activation free energy for the enantiomerization process, and the latter method the reliable values of activation enthalpy and entropy further supported by quantum-chemical calculations. Our calculations also revealed the individual internal rotations and structural deformations necessary for the enantiomerization of the helically chiral macrocycle to occur and confirmed thereby also that it follows *Mislow's* "Euclidian rubber glove" mechanism.

EXPERIMENTAL SECTION

Synthesis and Characterization. Experimental procedures and characterization data for all new compounds described in this work are compiled in the supporting information. All commercially available compounds were purchased from Sigma-Aldrich, Acros, Apollo Scientific, Alfa Aesar and Fluorochem and used without further purification. All reactions with reagents that are easily oxidized or hydrolyzed were performed under Argon using Schlenk techniques with anhydrous solvents in glassware, which was dried prior to use. The NMR experiments were performed at 400, 500 or 600 MHz proton frequencies. The instruments were equipped with a direct-observe 5 mm BBFO smart probe (400 and 600 MHz), an indirect-detection 5 mm BBI probe (500 MHz), or a five-channel cryogenic 5 mm QCI probe (600 MHz). All probes were equipped with actively shielded z-gradients (10 A). The chemical shifts are reported in ppm relative to tetramethylsilane or referenced to residual solvent peak and the J values are given in Hz (±0.1 Hz). The HPLC separation of the enantiomers of **1** was performed on an HPLC instrument equipped with a diode array UV-Vis detector (λ = 200 – 600 nm). The used column for separation on chiral stationary phase was a Chiralpak IG, 5 μm, 4.6 x 250 mm, Daicel Chemical Industries Ltd. The samples for CD spectra were eluted in *n*-hexane/EtOAc 4:1, the VT-HPLC studies were performed in *n*-hexane/EtOAc 2:1, flow rate 1.0 mL min^{-1}. The CD spectra were measured in a precooled 1 cm quartz glass cuvette directly after chiral HPLC at 283 K. All EXSY NMR experiments were performed on a Bruker Avance III NMR spectrometer operating at 600.13 MHz proton frequency. The instrument was equipped with an indirect 5-mm BBI probe with z-gradient. The experiments were performed between 373 and 393 K and the temperature was calibrated using a glycerol standard showing accuracy within +/- 0.2 K. Temperature equilibration was achieved after 20 min and only then the EXSY experiments were performed. The mixing times were set to 1000, 500 or 250 ms and the total experiment varied between 68 and 94 min. Manual integration of the EXSY cross peaks, normalized with the diagonal peaks yielded the rate constants which were determined applying the initial rate approximation. Eyring analysis of these rates yielded the enthalpic and entropic contributions to the activation energy.

DFT Calculations. The Gaussian 09 (release D01) program suite was used in all calculations.[35] The potential energy surface scans were performed at either semi-empirical PM6 or B3LYP/6-31G(d)

level of theories. The full gas phase geometry optimizations were done with B3LYP functional and 6-31G(d) basis set, and the character of the stationary point reached was confirmed by a subsequent frequency calculation. The zero-point vibrational energy correction obtained this way was used unscaled. The electronic circular dichroism spectra were obtained at CAM-B3LYP/cc-pVDZ level of theory calculating the first 75 electronic transitions. The velocity form of the rotatory strength was used. Empirical vibrational broadening for the electronic transitions was assumed (0.16 eV) and the position of the absorption bands was empirically shifted by +20 nm to match the energy of the first electronic transition. The ECD spectra were simulated in SpecDis (v1.71).[36]

ASSOCIATED CONTENT

Synthetic procedures and analytical data for all new compounds, HPLC, CD, crystallographic data, results of DFT calculations, ^{1}H and ^{13}C-NMR and HRMS spectra are supplied as Supporting Information. This material is available free of charge via the Internet at http://pubs.acs.org."

AUTHOR INFORMATION

Corresponding Author

* marcel.mayor@unibas.ch

Author Contributions

The manuscript was written through contributions of all authors. All authors have given approval to the final version of the manuscript.

REFERENCES

(1)   Rickhaus, M.; Mayor, M.; Juríček, M. Strain-Induced Helical Chirality in Polyaromatic Systems. *Chem Soc Rev* **2016**, *45*, 1542–1556.

(2)   Berezhnaia, V.; Roy, M.; Vanthuyne, N.; Villa, M.; Naubron, J.-V.; Rodriguez, J.; Coquerel, Y.; Gingras, M. Chiral Nanographene Propeller Embedding Six Enantiomerically Stable [5]Helicene Units. *J. Am. Chem. Soc.* **2017**, *139*, 18508–18511.

(3)   Fujikawa, T.; Preda, D. V.; Segawa, Y.; Itami, K.; Scott, L. T. Corannulene–Helicene Hybrids: Chiral π-Systems Comprising Both Bowl and Helical Motifs. *Org. Lett.* **2016**, *18*, 3992–3995.

(4)   Schuster, N. J.; Paley, D. W.; Jockusch, S.; Ng, F.; Steigerwald, M. L.; Nuckolls, C. Electron Delocalization in Perylene Diimide Helicenes. *Angew. Chem. Int. Ed.* **2016**, *55*, 13519–13523.

(5)   Gohler, B.; Hamelbeck, V.; Markus, T. Z.; Kettner, M.; Hanne, G. F.; Vager, Z.; Naaman, R.; Zacharias, H. Spin Selectivity in Electron Transmission Through Self-Assembled Monolayers of Double-Stranded DNA. *Science* **2011**, *331*, 894–897.

(6)   Iyoda, M.; Yamakawa, J.; Rahman, M. J. Conjugated Macrocycles: Concepts and Applications. *Angew. Chem. Int. Ed.* **2011**, *50*, 10522–10553.

(7)   Brown, C. J.; Farthing, A. C. Preparation and Structure of Di-p-Xylylene. *Nature* **1949**, *164*, 915–916.

(8)   Cram, D. J.; Steinberg, H. Macro Rings. I. Preparation and Spectra of the Paracyclophanes. *J. Am. Chem. Soc.* **1951**, *73*, 5691–5704.

(9)   Hinrichs, H.; Boydston, A. J.; Jones, P. G.; Hess, K.; Herges, R.; Haley, M. M.; Hopf, H. Phane Properties of [2.2]Paracyclophane/Dehydrobenzoannulene Hybrids. *Chem. - Eur. J.* **2006**, *12*, 7103–7115.

(10)   Morisaki, Y.; Gon, M.; Sasamori, T.; Tokitoh, N.; Chujo, Y. Planar Chiral Tetrasubstituted [2.2]Paracyclophane: Optical Resolution and Functionalization. *J. Am. Chem. Soc.* **2014**, *136*, 3350–3353.

(11)   Stefani, D.; Weiland, K. J.; Skripnik, M.; Hsu, C.; Perrin, M. L.; Mayor, M.; Pauly, F.; van der Zant, H. S. J. Large Conductance Variations in a Mechanosensitive Single-Molecule Junction. *Nano Lett.* **2018**, *18*, 5981–5988.

(12)   Weiland, K. J.; Münch, N.; Gschwind, W.; Häussinger, D.; Mayor, M. A Chiral Macrocyclic Oligothiophene with Broken Conjugation - Rapid Racemization through Internal Rotation. *Helv. Chim. Acta* **2018**, *101*, e1800205.

(13)   Flapan, E. *When Topology Meets Chemistry: A Topological Look at Molecular Chirality*; Outlooks; Cambridge University Press ; Mathematical Association of America: Cambridge ; New York : Washington, DC, **2000**.

(14)   Chambron, J.-C.; Sauvage, J.-P.; Mislow, K.; De Cian, A.; Fischer, J. A [2]Catenane and a [2]Rotaxane as Prototypes of Topological and Euclidean Molecular "Rubber Gloves." *Chem. - Eur. J.* **2001**, *7*, 4085–4096.

(15)   Mislow, K. Limitations of the Symmetry Criteria for Optical Inactivity and Resolvability *Science* **1954**, *120*, 232–233.

(16)   Vorontsova, N. V.; Rozenberg, V. I.; Sergeeva, E. V.; Vorontsov, E. V.; Starikova, Z. A.; Lyssenko, K. A.; Hopf, H. Symmetrically Tetrasubstituted [2.2]Paracyclophanes: Their Systematization and Regioselective Synthesis of Several Types of Bis-Bifunctional Derivatives by Double Electrophilic Substitution. *Chem. - Eur. J.* **2008**, *14*, 4600–4617.

(17)   Krömer, J.; Rios-Carreras, I.; Fuhrmann, G.; Musch, C.; Wunderlin, M.; Debaerdemaeker, T.; Mena-Osteritz, E.; Bäuerle, P. Synthesis of the First Fullyα-Conjugated Macrocyclic Oligothiophenes: Cyclo[n]Thiophenes with Tunable Cavities in the Nanometer Regime. *Angew. Chem.* **2000**, *39*, 3481–3486.

(18)   Mishra, A.; Ma, C.-Q.; Bäuerle, P. Functional Oligothiophenes: Molecular Design for Multidimensional Nanoarchitectures and Their Applications . *Chem. Rev.* **2009**, *109*, 1141–1276.

(19)   Le Pleux, L.; Kapatsina, E.; Hildesheim, J.; Häussinger, D.; Mayor, M. A Molecular Turnstile as an *E*-Field-Triggered Single-Molecule Switch: Concept and Synthesis: A Molecular Turnstile as an *E*-Field-Triggered Single-Molecule Switch: Concept and Synthesis. *Eur. J. Org. Chem.* **2017**, *2017*, 3165–3178.

(20)   Thirion, D.; Poriel, C.; Métivier, R.; Rault-Berthelot, J.; Barrière, F.; Jeannin, O. Violet-to-Blue Tunable Emission of Aryl-Substituted Dispirofluorene-Indenofluorene Isomers by Conformationally-Controllable Intramolecular Excimer Formation. *Chem. - Eur. J.* **2011**, *17*, 10272–10287.

(21)   Corey, E. J.; Fuchs, P. L. A Synthetic Method for Formyl -> Ethynyl Conversion. *Tetrahedron Lett.* **1972**, *13*, 3769–3772.

(22)   Morisaki, Y.; Kawakami, N.; Shibata, S.; Chujo, Y. Through-Space Conjugated Molecular Wire Comprising Three π-Electron Systems. *Chem. - Asian J.* **2014**, *9*, 2891–2895.

(23)   Gon, M.; Morisaki, Y.; Sawada, R.; Chujo, Y. Synthesis of Optically Active, X-Shaped, Conjugated Compounds and Dendrimers Based on Planar Chiral [2.2]Paracyclophane, Leading to Highly Emissive Circularly Polarized Luminescence. *Chem. - Eur. J.* **2016**, *22*, 2291–2298.

(24)   Yanai, T.; Tew, D. P.; Handy, N. C. A New Hybrid Exchange–Correlation Functional Using the Coulomb-Attenuating Method (CAM-B3LYP). *Chem. Phys. Lett.* **2004**, *393*, 51–57.

(25)   Bruhn, T.; Schaumlöffel, A.; Hemberger, Y.; Bringmann, G. SpecDis: Quantifying the Comparison of Calculated and Experimental Electronic Circular Dichroism Spectra: UV AND ECD EVALUATION WITH SPECDIS. *Chirality* **2013**, *25*, 243–249.

(26)   Trapp, O. A Novel Software Tool for High Throughput Measurements of Interconversion Barriers: DCXplorer☆. *J. Chromatogr. B* **2008**, *875*, 42–47.

(27)   D'Acquarica, I.; Gasparrini, F.; Pierini, M.; Villani, C.; Zappia, G. Dynamic HPLC on Chiral Stationary Phases: A Powerful Tool for the Investigation of Stereomutation Processes. *J. Sep. Sci.* **2006**, *29*, 1508–1516.

(28)   Rizzo, S.; Benincori, T.; Bonometti, V.; Cirilli, R.; Mussini, P. R.; Pierini, M.; Pilati, T.; Sannicolò, F. Steric and Electronic Effects on the Configurational Stability of Residual Chiral Phosphorus-Centered Three-Bladed Propellers: Tris-Aryl Phosphanes. *Chem. - Eur. J.* **2013**, *19*, 182–194.

(29)   Bihlmeier, A.; Rotzler, J.; Rickhaus, M.; Mayor, M.; Klopper, W. Activation Enthalpies and Entropies of the Atropisomerization of Substituted Butyl-Bridged Biphenyls. *Phys. Chem. Chem. Phys.* **2015**, *17*, 11165–11173.

(30)   Even with the solubilizing hexyl chains reduced to methyl groups or hydrogen atoms.

(31)   Although the dihedral angles between the plane of each of the thiophene units and the plane of the top or the bottom benzene ring of the PC, respectively, are not necessarily identical, a single variable α had to be used to simulate the PC rotation to avoid rotation of the thiophene unit when a single dihedral angle was constrained, while the other relaxed in the optimization.

(32)   The B3LYP PES calculations for both rotations overestimate the activation energy of each process. Therefore, both were corrected by the difference of the activation barrier obtained from the PES calculated for methyl benzoate and methyl formate at the same level of theory and the experimental values reported in the literature (refs. 33 and 34).

(33)   Bailey, J.; North, A. M. Ultrasonic Relaxation in Some Alkyl Esters. *Trans. Faraday Soc.* **1968**, *64*, 1499.

(34)   Pawar, D. M.; Wilson, K. K.; Noe, E. A. Barrier to Rotation about the Phenyl–Carbonyl Carbon Bond of Methyl Benzoate by Dynamic NMR Spectroscopy and Ab Initio Molecular Orbital Calculations. *J. Org. Chem.* **2000**, *65*, 1552–1553.

(35)   Frisch, M. J.; Trucks, G. W.; Schlegel, H. B.; Scuseria, G. E.; Robb, M. A.; Cheeseman, J. R.; Scalmani, G.; Barone, V.; Petersson, G. A.; Nakatsuji, H.; Li, X.; Caricato, M.; Marenich, A. V.; Bloino, J.; Janesko, B. G.; Gomperts, R.; Mennucci, B.; Hratchian, H. P.; Ortiz, J. V.; Izmaylov, A. F.; Sonnenberg, J. L.; Williams-Young, D.; Ding, F.; Lipparini, F.; Egidi, F.; Goings, J.; Peng, B.; Petrone, A.; Henderson, T.; Ranasinghe, D.; Zakrzewski, V. G.; Gao, J.; Rega, N.; Zheng, G.; Liang, W.; Hada, M.; Ehara, M.; Toyota, K.; Fukuda, R.; Hasegawa, J.; Ishida, M.; Nakajima, T.; Honda, Y.; Kitao, O.; Nakai, H.; Vreven, T.; Throssell, K.; Montgomery, J. A., Jr.; Peralta, J. E.; Ogliaro, F.; Bearpark, M. J.; Heyd, J. J.; Brothers, E. N.; Kudin, K. N.; Staroverov, V. N.; Keith, T. A.; Kobayashi, R.; Normand, J.; Raghavachari, K.; Rendell, A. P.; Burant, J. C.; Iyengar, S. S.; Tomasi, J.; Cossi, M.; Millam, J. M.; Klene, M.; Adamo, C.; Cammi, R.; Ochterski, J. W.; Martin, R. L.; Morokuma, K.; Farkas, O.; Foresman, J. B.; Fox, D. J. Gaussian 09, Revision D.01, Gaussian, Inc., Wallingford CT, 2009.

(36)   Bruhn, T.; Schaumlöffel, A.; Hemberger, Y; Bringmann, G. SpecDis: Quantifying the Comparison of Calculated and Experimental Electronic Circular Dichroism Spectra. *Chirality* **2013**, *25*, 243–249.

Journal of the American Chemical Society

Insert Table of Contents artwork here